CHEMISTRY
AN ASIAN JOURNAL

DOI: 10.1002/asia.201200627

Selective Pyrophosphate Recognition by Cyclic Peptide Receptors in Physiological Saline

Stephen J. Butler and Katrina A. Jolliffe*[a]

Abstract: The anion binding ability of a family of bis(Zn^{II}-Dpa) functionalized cyclic peptides has been investigated using displacement assays with a fluorescent coumarin indicator in water, saline solution, and Krebs buffer. Nonbinding side-chain steric bulk, the relative position of binding sites, and the scaffold size were all found to affect the ability of these receptors to discriminate between polyphosphate ions. Most receptors showed some selectivity for pyrophosphate over ATP and ADP in water and saline, and this selectivity was significantly enhanced in the biologically relevant Krebs buffer giving chemosensing ensembles capable of selective recognition of pyrophosphate in the presence of excess ATP.

Keywords: anions · molecular recognition · peptides · receptors · supramolecular chemistry

Introduction

Anions are involved in almost every biological process, with phosphates amongst the most important anions in the natural world. They are involved in bioenergetic and metabolic processes and can be either substrates for, or products of, enzyme-catalyzed reactions. For example, hydrolysis of anionic ATP results in the formation of both pyrophosphate ($P_2O_7^{4-}$, PPi) and AMP anions. PPi is also released when nucleoside triphosphates are incorporated into DNA/RNA during polymerase reactions and in the biosynthesis of secondary messengers such as cAMP and cGMP.[1] Elevated levels of PPi in synovial fluid have been found in patients with pseudogout and osteoarthritis,[2] and the levels of PPi in urine can be used to monitor clinical disorders in bone metabolism[3] and urolithiasis.[4] Therefore, there has been significant recent interest in the development of molecular receptors capable of discriminating between PPi and other phosphate derivatives, for use in bioanalytical assays.[5–9] The major challenges in the development of sensors for PPi for use in bioanalytical applications are the development of molecules capable of recognition of these highly hydrated anions[10] in a complex physiological environment, where numerous competing analytes and proteins are present, and the development of receptors capable of discriminating between PPi and nucleoside triphosphates, which have an identical charge.[6,8] While there has been significant recent progress in the development of sensors capable of binding PPi in aqueous solution, very few are capable of distinguishing PPi from the nucleoside triphosphates with a useful level of discrimination[9,11] and few have been evaluated under 'real' physiological conditions such as cell growth media.

We have previously reported the use of a backbone-modified cyclic peptide bearing dipicolylamino (Dpa) arms as a selective receptor for PPi ions in water as determined using a fluorescent indicator displacement assay (IDA).[11] One of the advantages of peptide-derived receptors is their synthetic versatility, which allows each subunit of the receptor to be modified, enabling ready fine-tuning of the receptor properties.[12,13] We have recently illustrated how this approach can be used to prepare a small library of cyclic peptide anion receptors (**1–6·Zn_2**, Figure 1)[14,15] and report here on the ability of these receptors to bind PPi in aqueous solution and physiological saline (Krebs buffer; commonly used for cell and tissue culture and approximately isotonic with blood serum[16]) with high levels of selectivity over ATP and ADP.

Results and Discussion

Synthesis and Characterization of the Cyclic Peptide Receptor

Based on previous studies,[11,14,17] we designed a series of receptors **1–6·Zn_2** to probe the effects that 1) spacing between the two Zn^{II}Dpa binding sites, 2) steric bulk of the 'nonbinding' side chains, and 3) size of the cyclic peptide scaffold would have on anion binding affinity and selectivity. The synthesis of C_2-symmetric receptors **1·Zn_2**-**3·Zn_2** and unsymmetrical receptors **4·Zn_2**-**5·Zn_2** was described previously.[11,14] The smaller receptor **6·Zn_2**, based on a hexapeptide scaffold, was synthesized using solid-phase peptide synthesis (SPPS) followed by macrocyclization and functionalization in a manner similar to the other systems. Briefly, the linear precursor to cyclic peptide **6** was prepared on 2-chlorotrityl chloride resin, using Fmoc/HATU chemistry to couple the

[a] Dr. S. J. Butler, Prof. Dr. K. A. Jolliffe
School of Chemistry (Building F11)
The University of Sydney
NSW, 2006, Australia
Fax: (+61) 2-9351-3329
E-mail: kate.jolliffe@sydney.edu.au

Supporting information for this article is available on the WWW under http://dx.doi.org/10.1002/asia.201200627.

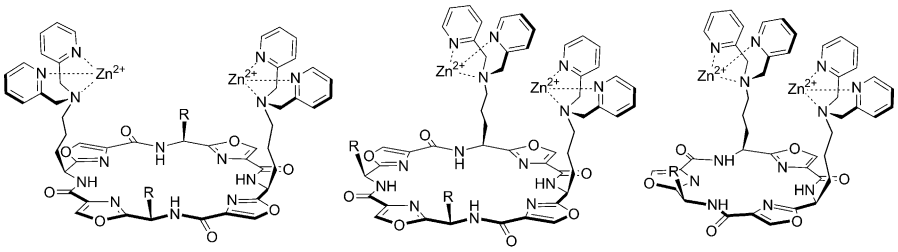

Figure 1. Series of cyclic peptide-based receptors **1**–**6·Zn$_2$**.

ornithine- and leucine-derived building blocks, which have been previously reported.[14] The linear peptide was cleaved from the resin using mildly acidic conditions to give **7** in approximately 75% yield (based on reversed-phase HPLC analysis). Cyclization of **7** was effected using the coupling reagent 4-(4,6-dimethoxy-1,3,5-triazin-2-yl)-4-methylmorpholinium tetrafluoroborate (DMTMM)[18] in the presence of Hünig's base to afford the desired cyclic peptide **8** in 32% yield. The Cbz protecting groups of cyclic peptide **8** were removed using a solution of 45% hydrogen bromide in acetic acid giving the diamine **9** upon a basic work-up procedure. Afterwards, **9** was subjected to reductive amination with 2-pyridinecarboxaldehyde using our previously established conditions,[11] thus providing the Dpa-functionalized cyclic peptide **6** in 76% yield over two steps. Subsequent addition of two equivalents of $Zn(NO_3)_2$ gave the fully-functionalized anion receptor **6·Zn$_2$** (Scheme 1).

Anion Binding Studies

In order to determine the anion binding capabilities of **1**–**6·Zn$_2$**, we employed indicator displacement assays[19] using the previously reported fluorescent coumarin derivative **10**.[11,14,20] Our initial studies were performed in 5 mM HEPES buffer at pH 7.4, as all receptors were soluble in this medium. Titration of solutions of **1**–**6·Zn$_2$** into a solution of **10** (10 μM, pH 7.4, 25 °C) resulted in concentration-dependent quenching of the indicator fluorescence (a 4.5-fold decrease in fluorescence intensity upon addition of 1 equiv of **1**–**6·Zn$_2$** was observed in all cases, with quenching reaching a maximum upon addition of 2 equiv of **1**–**6·Zn$_2$**). A shift in the emission maximum from 480 nm to 530 nm was also observed, as well as a pseudo-isosbestic point at 568 nm, thus indicating that the indicator–receptor complexes were the predominant species in solution (Figure 2). All receptors bound **10** strongly [log K_{in} = 6.2–7.3 (±0.1)], as determined by nonlinear least-squares curve fitting of the titration data to a 1:1 binding model[21] (the stoichiometry was confirmed by the mole-ratio method[22] for all receptors and additionally using Job plots for receptors **1**[11] and **2**), with receptor **6·Zn$_2$** having the highest affinity for **10**.

Titration of 1:1 solutions of the indicator–receptor complexes (10 mM) with aliquots of the sodium salts of PPi, ATP, and ADP resulted in significant increases in fluorescence intensity indicating displacement of the indicator, while AMP, cAMP, phosphoserine, phosphotyrosine, hydrogenphosphate (Figure 3), and the polycarboxylates acetylglutamate and Ac-Glu-Gly-Glu (see the Supporting Information) were not able to displace the indicator from any of the receptors to an appreciable extent (<10% fluorescence recovery upon addition of 10 equiv hydrogenphosphate), thus indicating the selectivity of these receptors for di- and triphosphate anions over monophosphate anions and polycarboxylates. Addition of 1 equivalent of PPi resulted in almost complete restoration of the fluorescence intensity, while the addition of ATP or ADP resulted in 4-fold and 3.5-fold fluorescence enhancements, respectively.

Fluorescence emission intensities (λ_{ex} = 347 nm, λ_{em} = 480 nm) from these titrations were analyzed using a curve-fitting procedure based on the equilibria previously described for competition assays,[23] with our pre-determined values for K_{in} to determine the apparent stability constants (Table 1). The assumed 1:1 binding mode was supported by mass spectrometric data of the PPi-receptor complexes, in which the major signals observed corresponded to the singly charged PPi complexes [receptor + PPi + H]$^+$ (see the Supporting Information).

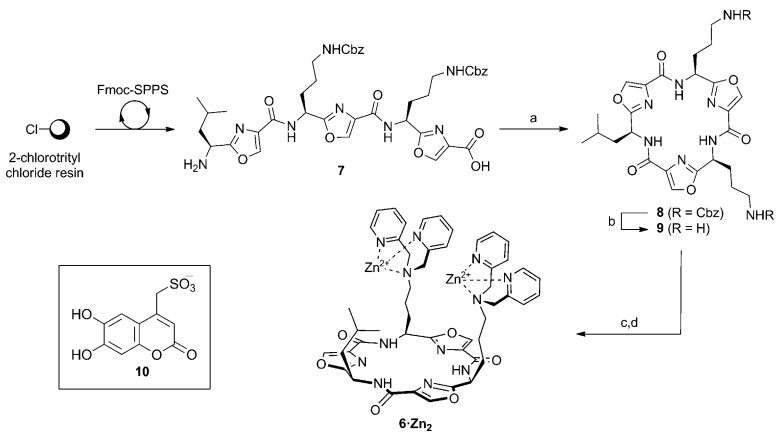

Scheme 1. Solid-phase synthesis of receptor **6·Zn$_2$** and structure of indicator **10** (inset). Conditions: a) DMTMM (3 equiv), Hünig's base (5 equiv), DMF (0.05 M); b) 45% HBr in AcOH, followed by basic work-up with 0.3 M NaOH; c) 2-pyridinecarboxaldehyde (20 equiv), $NaHB(OAc)_3$ (20 equiv), DMF; d) $Zn(NO_3)_2 \cdot 4H_2O$ (2 equiv), CD_3OD.

CHEMISTRY
AN ASIAN JOURNAL

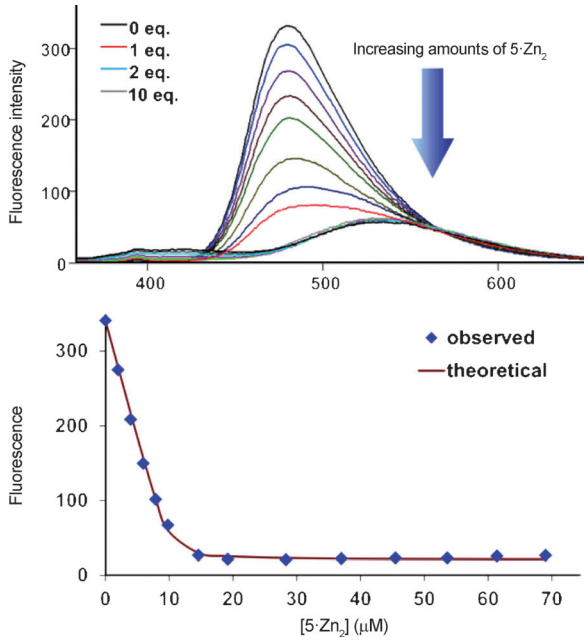

Figure 2. Representative spectra showing the change in fluorescence emission of indicator **10** (10 μM) upon the addition of increasing amounts of receptor **5·Zn$_2$** (top); change in fluorescence intensity of **10** (10 μM) at 480 nm upon the addition of increasing amounts of receptor **5·Zn$_2$** (bottom). Measurement conditions: aqueous solution of HEPES buffer (5 mM, pH 7.4), $\lambda_{ex}=347$ nm, 25 °C.

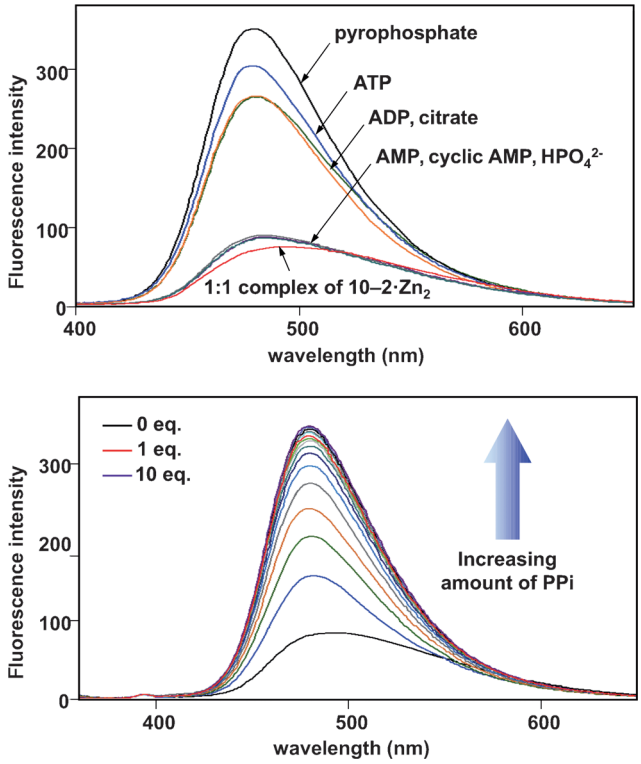

Figure 3. Representative change in fluorescence emission of the complex **10-2·Zn$_2$** (10 μM) upon the addition of: (top) 10 equivalents of various anions (sodium salts), and (bottom) 10 equivalents of pyrophosphate (sodium salt) in incremental steps. Measurement conditions: aqueous solution of HEPES buffer (5 mM, pH 7.4), $\lambda_{ex}=347$ nm, 25 °C.

Table 1. Apparent association constants (log K_a) determined for receptors **1–6·Zn$_2$** and various polyphosphate anions in aqueous solution (5 mM HEPES, pH 7.4).

Anion	**1·Zn$_2$**	**2·Zn$_2$**	**3·Zn$_2$**	**4·Zn$_2$**	**5·Zn$_2$**	**6·Zn$_2$**
Indicator **10**	6.3	6.2	6.9	6.9	6.8	7.3
PPi	7.2	7.4	8.4	8.8	7.9	9.8
ATP	6.5	7.6	8.6	8.3	7.2	9.1
ADP	6.3	7.4	7.5	7.7	7.0	7.9

Each value represents the average of at least two separate titration experiments. Errors < 10 %.

Notably, significant differences in binding affinity and selectivity were observed between members of the family of receptors. Comparing binding data for the series **1–3·Zn$_2$**, in which the steric bulk of the non-binding side chains is altered, indicates that while the hydrophobic cleft provided by the Leu side chains of **2·Zn$_2$** results in similar affinity for all three anions [log K_a 7.4–7.6 (±0.2)], the smaller Ala substituents of **1·Zn$_2$** provide some selectivity for PPi over ATP and ADP. In contrast, for **3·Zn$_2$** in which the non-binding substituents are Phe side chains, binding is in the order ATP ≈ PPi > ADP. Molecular models (SPARTAN 06, MMFF94) of the complexes of **3·Zn$_2$** with ATP and ADP suggest that the reason for the increased affinity of this receptor for ATP may be a result of a secondary π–π interaction between one of the Phe residues and the adenine moiety of ATP. In contrast, the backbone of ADP is too short to allow this interaction to occur (Figure 4).

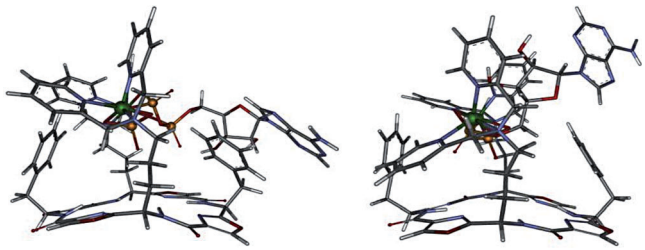

Figure 4. Molecular structures of: (left) the ATP complex of receptor **3·Zn$_2$**, and (right) the ADP complex of receptor **3·Zn$_2$**, modelled using SPARTAN 06 (MMFF94).

Moving the Zn^{II}Dpa sites closer together on the scaffold resulted in increased selectivity for PPi over ATP and ADP in both the Phe and Leu series. Notably, the affinity of **4·Zn$_2$** (which has proximal Zn^{II}Dpa side chains) for PPi is more than an order of magnitude higher than that of **2·Zn$_2$**, in which the Dpa side chains are distal, while for **5·Zn$_2$** affinity for all three anions drops slightly in comparison to that of **3·Zn$_2$**. Surprisingly, changing the size of the cyclic peptide scaffold while maintaining the same distance between the binding sites had a significant effect on binding affinity with **6·Zn$_2$** binding PPi an order of magnitude more strongly than **4·Zn$_2$** and with increased selectivity over both ATP and ADP. Since the Zn^{II}Dpa binding sites are expected to be at almost identical distances apart in **4·Zn$_2$** and **6·Zn$_2$**, this difference in binding affinity might reflect reduced steric inter-

ference from the single Leu side chain in **6·Zn$_2$** compared to the two bulky side chains present in **4·Zn$_2$**.

These initial binding studies revealed that selectivity between di- and triphosphate anions can be modulated by changing both the nature and position of the non-binding side chains in receptors **1**–**6·Zn$_2$**, as well as the size of the cyclic peptide scaffold. Next, we investigated the binding properties of the receptors in a medium that closely mimics physiological conditions (i.e., aqueous solution, pH 7.4, 154 mM NaCl). It should be noted that, in a saline solution, the high concentration of chloride anions may provide competition for the anion binding sites. In addition, sodium and chloride ions may interfere with the IDA by quenching the fluorescence of coumarin indicator **10**.[24]

Titrations of each of the receptors **1·Zn$_2$**, **2·Zn$_2$**, **4·Zn$_2$**, and **6·Zn$_2$** into aqueous solutions of indicator **10** (10 μM, 5 mM HEPES, pH 7.4, 145 mM NaCl, 25 °C) resulted in quenching of fluorescence emission of the indicator in a concentration-dependent manner (Figure 5). The addition of one equivalent of each receptor gave rise to a 2-fold decrease in fluorescence intensity. Receptors **3·Zn$_2$** and **5·Zn$_2$**, bearing phenylalanine residues, were insoluble in the saline solution and were not tested under these conditions. The titration data were analyzed using a 1:1 binding model (Figure 5, inset) as described previously, giving association constants in the range log K_{in} = 5.4–5.8 (±0.1) (Table 2). As expected, each receptor displayed a lower affinity for indicator **10** under these conditions as compared to those determined in the absence of NaCl. The association constant determined for the binding of indicator **10** to receptor **1·Zn$_2$** was in agreement with the previously reported log K_{in} value of 5.1 ± 0.1, which was determined at a slightly lower pH of 7.2.[11]

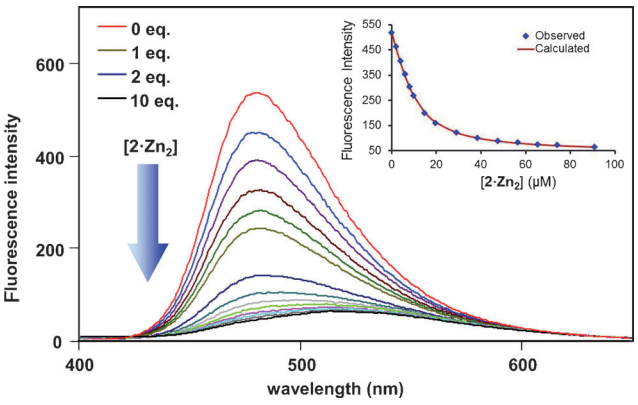

Figure 5. Representative change in fluorescence emission of indicator **10** (10 μM) upon the addition of increasing amounts of receptor **2·Zn$_2$**. Inset: change in fluorescence intensity of **10** (10 μM) at 480 nm upon increasing amounts of receptor **2·Zn$_2$**. Measurement conditions: aqueous solution of 5 mM HEPES (pH 7.4) containing 145 mM NaCl, λ_{ex} = 347 nm, 25 °C.

Subsequent competition assays revealed that each of the receptors retain their selectivity for di- and triphosphate anions over monophosphate derivatives in a saline solution. Pyrophosphate, ATP, and ADP were capable of competitive displacement of the indicator from each of the 1:1 indicator–receptor complexes, as demonstrated by large enhancements in fluorescence emission (Figure 6). By contrast, none of the monophosphate derivatives were able to displace the indicator by a significant amount. Apparent association constants between each of the receptors and PPi, ATP, and ADP are given in Table 2. As expected, the receptors showed slightly lower affinity for all three anions in a saline solution as compared to that determined in the absence of NaCl, with similar patterns of selectivity to those observed in 5 mM HEPES buffer above.

Table 2. Apparent association constants (log K_a) determined for receptors **1·Zn$_2$**, **2·Zn$_2$**, **4·Zn$_2$**, and **6·Zn$_2$** and various polyphosphate anions in aqueous solution (5 mM HEPES, pH 7.4, 145 mM NaCl).

Anion	**1·Zn$_2$**	**2·Zn$_2$**	**4·Zn$_2$**	**6·Zn$_2$**
Indicator **10**	5.5	5.4	5.6	5.8
PPi	6.8	6.4	7.5	7.9
ATP	6.3	6.4	6.1	6.8
ADP	6.0	6.4	6.3	6.2

Each value represents the average of at least two separate titration experiments. Errors < 10 %.

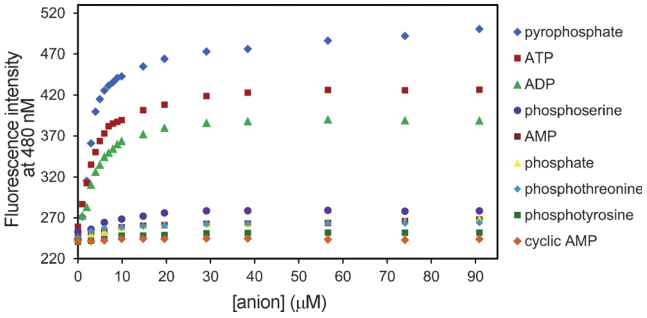

Figure 6. Change in fluorescence intensity (at 480 nm) of the complex **10**-**2·Zn$_2$** upon addition of various phosphate oxoanions (sodium salts). Measurement conditions: aqueous solution (5 mM HEPES, pH 7.4, 145 mM NaCl), λ_{ex} = 347 nm, 25 °C.

In order to utilize these complexes in a biological assay, such as for the detection of PPi in extracellular fluid or urine, they must be functional in a medium that contains both a large excess of anions (chloride and phosphate) as well as numerous other species such as metal ions that could potentially interfere with the recognition process. Therefore, we assessed the binding capabilities of receptors **1·Zn$_2$**, **2·Zn$_2$**, **4·Zn$_2$**, and **6·Zn$_2$** towards PPi, ATP, and ADP in a Krebs buffer solution, which is commonly used for cell and tissue culture in biological research. Krebs buffer (composition: 137 mM NaCl, 5.4 mM KCl, 1.2 mM $MgSO_4$, 2.8 mM $CaCl_2$, 0.4 mM KH_2PO_4, 0.3 mM NaH_2PO_4, 10 mM Tris base, 10 mM glucose, buffered to pH 7.4) contains high concentrations of phosphate anions (700 μM) and Ca^{2+} and Mg^{2+} ions, both of which are known to bind strongly to PPi, ATP, and ADP.[25–27] Using fluorescence titrations, we determined that all four receptors bind indicator **10** with similar affinities (log K_as 5.1–5.4) to those determined above in NaCl/

CHEMISTRY
AN ASIAN JOURNAL

HEPES buffer solution, thereby indicating that the additional species in Krebs buffer should not interfere with the displacement assay (Figure 7).

Remarkably, competition assays in Krebs buffer indicated that selectivity of the chemosensing ensembles for PPi over

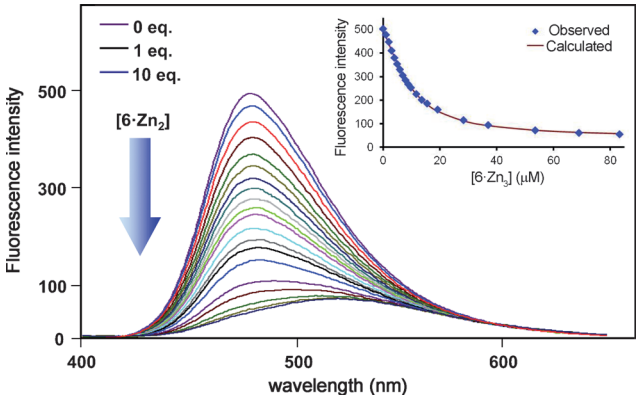

Figure 7. Representative change in fluorescence emission of indicator **10** (10 μM) in Krebs buffer upon the addition of increasing amounts of receptor **6·Zn$_2$**. Inset: change in fluorescence intensity of **10** (10 μM) at 480 nm upon addition of receptor **6·Zn$_2$**. Measurement conditions: aqueous solution of Krebs buffer (pH 7.4), λ_{ex} = 347 nm, 25 °C.

ATP and ADP was enhanced in this more complex medium. In particular, ensemble **10-6·Zn$_2$** showed a remarkable ability to discriminate between PPi and ATP/ADP in Krebs buffer. Only PPi was able to completely displace the indicator from the receptor under these conditions, as demonstrated by full recovery of the fluorescence signal (Figure 8). Both ATP and ADP were unable to displace the indicator by a significant amount, giving minor yet reproducible fluorescence enhancements. Analysis of the titration data using the curve-fitting procedure described above indicated that in Krebs buffer **6·Zn$_2$** has a similar affinity for PPi to that observed in saline, although data did not fit as well to a 1:1 competitive binding model, reflecting the additional equilibria present between PPi and species such as Ca^{2+} and Mg^{2+}. The other chemosensing ensembles exhibited similar behavior. The notable improvement in selectivity for PPi over ATP and ADP in Krebs saline relative to NaCl solution is readily apparent from a comparison of the titration plots of ensemble **10–6·Zn$_2$** with these anions (Figure 9), thus illustrating the lack of fluorescence recovery afforded by ATP and ADP in Krebs saline. This improved selectivity enables low micromolar concentrations of PPi to be detected in the presence of 100 μM ATP (Figure 10), which should prove useful in monitoring enzymatic reactions in which PPi is generated.

Notably, all three phosphate derivatives are known to bind strongly and with similar affinity (slightly lower for ADP) to Mg^{2+} and Ca^{2+} ions (reported log K_a values at similar pH and ionic strength to those in the current study for $MgPPi^{2-}$ = 4.26,[25] Mg_2PPi = 2.59,[25] $MgATP^{2-}$ = 4.22,[25] $MgADP^{-}$ = 3.6,[26] $CaPPi^{2-}$ = 3.17,[27] $CaATP^{2-}$ = 3.18,[27] and

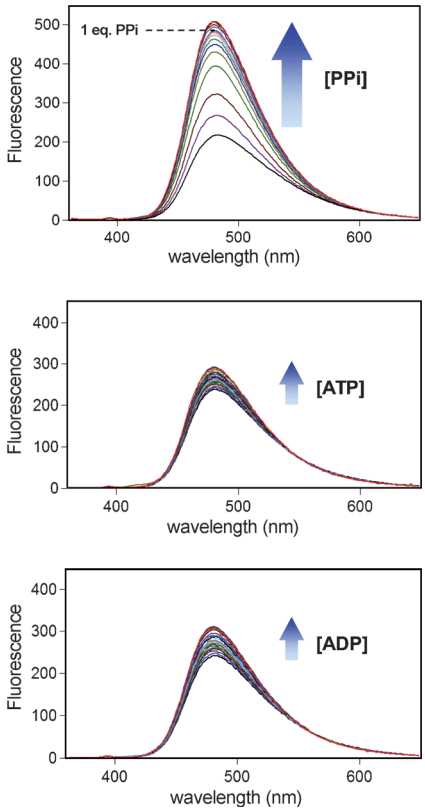

Figure 8. Representative change in fluorescence emission of the complex **10-6·Zn$_2$** (10 μM) in Krebs buffer upon the addition of 10 equivalents of: PPi (top), ATP (middle), and ADP (bottom). Measurement conditions: aqueous solution of Krebs buffer (pH 7.4), λ_{ex} = 347 nm, 25 °C.

$CaADP^{-}$ = 2.84[27]). Therefore, the enhanced selectivity observed for PPi over ATP (and ADP) in Krebs saline cannot be attributed to the difference in affinity of PPi and ATP for either Ca^{2+} or Mg^{2+} since both of these metal ions bind with similar affinity to the two phosphate derivatives. This suggests that the enhanced selectivity observed for PPi in Krebs solution is predominantly a result of the higher affinity for this ion by receptor **6·Zn$_2$** compared to ATP or ADP, resulting in both an increased ability of PPi to displace the indicator **10** from the receptor and increased competition between the receptor and metal ions for PPi. The numerous competitive equilibrium processes occurring in this complex mixture appear to be significantly affected by these differences in binding affinity, highlighting one of the advantages of indicator displacement assays for sensing purposes and suggesting that alternative indicators could also be employed to tune the affinity of the various chemosensing ensembles for different polyphosphate anions.

Conclusions

In summary, we have investigated the anion binding ability of a family of bis[Zn^{II}Dpa] functionalized cyclic peptides using indicator displacement assays and found that these flu-

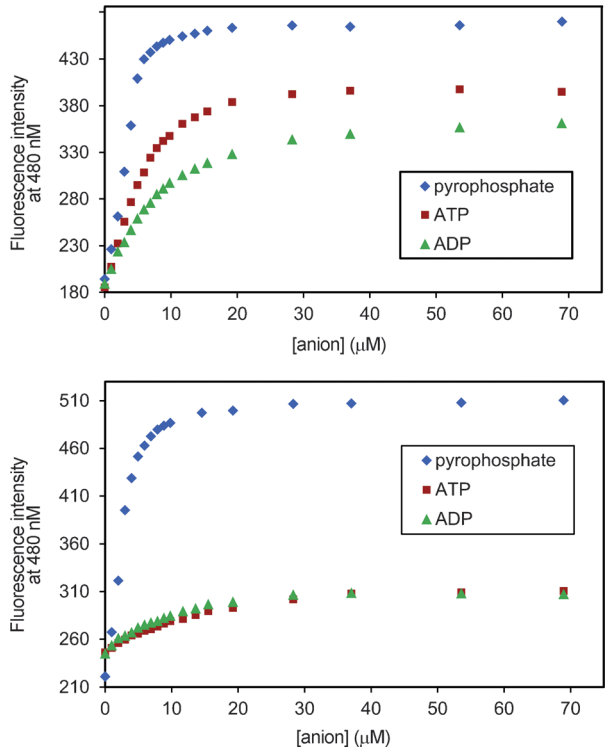

Figure 9. A comparison of the changes in fluorescence emission observed for the complex **10-6·Zn$_2$** (10 μM) upon the addition of various anions in: (top) saline solution and (bottom) Krebs buffer solution. Measurement conditions: pH 7.4, λ_{ex} = 347 nm, 25 °C.

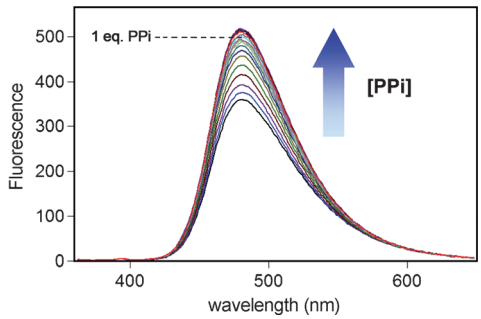

Figure 10. Change in fluorescence emission of **10-6·Zn$_2$** (10 μM) in Krebs buffer containing excess ATP (100 μM) upon the addition of 10 equivalents of PPi (0–100 μM). Measurement conditions: aqueous solution of Krebs buffer (pH 7.4), ATP (100 μM), λ_{ex} = 347 nm, 25 °C.

orescent chemosensing ensembles show excellent selectivity for PPi over ATP and ADP in Krebs buffer. Notably, selectivity for PPi is significantly enhanced in this biologically relevant medium compared to aqueous buffer, illustrating the importance of the composition of the medium and the presence of competing species in determining selectivity for anions, and suggesting that other receptors that bind anions with some selectivity in water should be reinvestigated in this biorelevant aqueous fluid. Use of the cyclic peptide scaffold has allowed an investigation of the effects of a number of features (binding site position, 'non-binding' side chain steric bulk, and scaffold size) on anion binding ability, enabling the tuning of the receptor to optimize selectivity for the analyte of interest (PPi). Current studies are focused on tuning the selectivity of these receptors for a variety of anions using a larger library of cyclic peptide scaffolds and alternative indicators for displacement assays.

Experimental Section

General methods and instrumentation used were identical to those reported previously.[14] Abbreviations used: dimethylformamide (DMF); *O*-(7-aza-1H-benzotriazole-1-yl)-*N*,*N*,*N*′,*N*′-tetramethyluronium hexafluorophosphate (HATU); 4-(4,6-dimethoxy-1,3,5-triazin-2-yl)-4-methylmorpholinium tetrafluoroborate (DMTMM); trifluoroacetic acid (TFA); reversed-phase high performance liquid chromatography (RP-HPLC).

General Procedures for Solid-Phase Peptide Synthesis

1. Loading of amino acid onto 2-chlorotrityl chloride resin: Under an atmosphere of nitrogen, 2-chlorotrityl chloride resin (resin capacity 1.01–1.4 mmol g^{-1}) was swollen in a sinter-fitted syringe in anhydrous dichloromethane for 1 h. The resin was drained and treated with a solution of Fmoc-protected amino acid (1.5 equiv relative to resin capacity) and Hünig's base (5 equiv relative to resin capacity) in anhydrous dichloromethane/DMF (9:1 *v*/*v*, 0.1 M) and the resulting suspension was gently agitated at rt for 24 h under an atmosphere of nitrogen. At this time the resin was drained and then treated with a mixture of methanol/Hünig's base/dichloromethane (2:1:17 *v*/*v*/*v*, 2×5 mL×15 min). The resin was then washed sequentially with DMF (2×10 mL), dichloromethane (3×10 mL), and diethyl ether (3×10 mL). The residual solvent was removed under reduced pressure.

2. *N*-terminal Fmoc deprotection: The resin-bound peptide was agitated in a solution of 10% piperidine in DMF (2×5 mL×15 min) and then drained and washed sequentially with DMF (2×5 mL), dichloromethane (3×5 mL), and DMF (3×5 mL). The resulting resin-bound amine was used immediately in the next peptide coupling step.

3. Estimation of resin loading: The drained Fmoc deprotection solution was diluted with a solution of 10% piperidine in DMF so that the maximum concentration of the fulvene-piperidine adduct was in the range of 2.5–7.5×10^{-5} M. A sample of this solution (2×3 mL) was transferred to two matched 1 cm quartz glass cuvettes and the UV/Vis absorbance at 301 nm was measured, using a solution of 10% piperidine in DMF as a reference. An average of the two absorbance values was used to calculate the loading, using ε = 7800 M^{-1} cm^{-1}.

4. SPPS Peptide coupling: Under an atmosphere of nitrogen, a solution of Fmoc-protected oxazole (1.5 equiv relative to loading), HATU (2 equiv relative to peptide) and Hünig's base (3 equiv relative to peptide) in anhydrous DMF (0.1 M relative to dipeptide) was added to the resin and the resulting suspension was agitated at rt for 24 h. The resin was then washed sequentially with DMF (2×5 mL), dichloromethane (3×10 mL), and DMF (3×5 mL).

5. Cleavage of peptides from the resin: A mixture of hexafluoroisopropanol/dichloromethane (1:4 *v*/*v*, 3×5 mL) was added to the resin and the resulting suspension was agitated at rt for 15 min. The solutions were drained and combined, and the solvent was removed under reduced pressure to afford the crude linear peptide.

Synthesis

*H_2N-Leu-Oxz(Ser)-[Orn(Cbz)-Oxz(Ser)]$_2$-OH (**7**)*

The oxazole building block Fmoc-Orn(Cbz)-Oxz(Ser)-OH[14] was loaded onto 2-chlorotrityl chloride resin (0.150 g, resin capacity 1.1 mmol g^{-1}) according to general procedure 1 (loading 0.88 mmol g^{-1}). Building blocks Fmoc-Orn(Cbz)-Oxz(Ser)-OH[14] and Fmoc-Leu-Oxz(Ser)-OH[14] were coupled sequentially to the resin-bound amine according to the SPPS

procedure 4 to give the resin-bound trioxazole. The *N*-terminal Fmoc protecting group was removed (general procedure 2), and the resulting amine was cleaved from the resin (general procedure 5) to afford H_2N-Leu-Oxz(Ser)-[Orn(Cbz)-Oxz(Ser)]$_2$-OH (**7**) (138 mg, quant.) as a colorless solid, which was used in the next step without further purification. LRMS (ESI) $m/z = 829$ $[M+H]^+$.

*Cyclo-Leu-Oxz(Ser)-[Orn(Cbz)-Oxz(Ser)]$_2$ (**8**)*

To a solution of the linear trioxazole **7** (138 mg, 0.132 mmol) in anhydrous DMF (0.05 M) was added DMTMM (3 equiv) and Hünig's base (5 equiv), and the resulting mixture was stirred at rt for 72 h under an atmosphere of nitrogen. The mixture was acidified by the addition of hydrochloric acid (0.3 M, pH 5) and then partitioned between water (20 mL) and chloroform/isopropanol (3:1 *v*/*v*, 20 mL). The aqueous phase was extracted with chloroform/isopropanol (3:1 *v*/*v*, 3×20 mL) and the combined organic fractions were dried ($MgSO_4$) and concentrated under reduced pressure to give a yellow oil. Subjection of the crude material to preparative RP-HPLC [gradient: 20–80 % acetonitrile (0.05 % TFA) in water (0.05 % TFA) over 50 min] gave the desired cyclic trioxazole **8** ($t_R = 50.5$ min, 34 mg, 32 %) as a colorless solid. $[\alpha]_D^{20} = -7.18$ ($c = 0.85$, MeOH); ^{1}H NMR (400 MHz, CD_3OD): $\delta = 0.95$ (d, $J = 6.4$ Hz, 3H), 1.02 (d, $J = 6.4$ Hz, 3H), 1.48 (m, 2H), 1.65 (m, 2H), 1.76 (m, 1H), 1.84 (m, 2H), 1.96 (m, 2H), 2.10 (m, 2H), 3.14 (t, $J = 6.6$ Hz, 4H), 5.02 (s, 4H), 5.22–5.30 (m, 3H), 7.23–7.33 (m, 10H), 8.42 (s, 2H), 8.44 ppm (s, 1H), N-H signals not observed; ^{13}C NMR (100.6 MHz, CD_3OD): $\delta = 22.9$, 23.1, 25.9, 26.3, 32.6, 32.7, 41.2, 45.4, 48.1, 67.3, 128.7, 128.9, 129.4, 136.2, 136.3, 138.4, 143.4, 143.6, 143.7, 158.9, 161.3, 161.4, 165.0(7), 165.1(3), 165.9 ppm, twelve signals obscured or overlapping; HRMS (ESI) calcd. for $C_{41}H_{46}N_8O_{10}Na$ $[M+Na]^+$ 833.3229, found 833.3203.

*Cyclo-Leu-Oxz(Ser)-[Orn(Dpa)-Oxz(Ser)]$_2$ (**6**)*

Step 1. A solution of hydrogen bromide in acetic acid (33 % *v*/*v*, 2.0 mL) was added to Cyclo-Leu-Oxz(Ser)-[Orn(Cbz)-Oxz(Ser)]$_2$ (**8**, 32 mg, 0.039 mmol), and the resulting mixture was stirred under nitrogen at rt for 24 h. Anhydrous ether (10 mL) was added to give a cream colored precipitate which was condensed by centrifugation. Subsequent trituration of the precipitate with anhydrous ether (10×10 mL) and removal of the final clear ethereal layer under reduced pressure gave the dihydrobromide salt as a cream colored solid. The crude material was partitioned between chloroform/isopropanol (3:1 *v*/*v*, 10 mL) and NaOH (0.3 M, 10 mL) and the aqueous phase was extracted with chloroform/isopropanol (3:1 *v*/*v*, 4×10 mL). The combined organic fractions were dried ($MgSO_4$) and concentrated under reduced pressure to give the crude diamine **9** as a colorless solid.

Step 2. To a degassed solution of the diamine **9** (0.039 mmol) in anhydrous DMF (2.0 mL) was added 2-pyridinecarboxaldehyde (20 equiv) and sodium triacetoxyborohydride (25 equiv), and the resulting mixture was stirred at 35 °C for 72 h. The mixture was concentrated to almost dryness and then partitioned between chloroform-isopropanol (3:1 *v*/*v*, 20 mL) and NaOH (0.3 M, pH 8). The aqueous phase was extracted with chloroform/isopropanol (3:1 *v*/*v*, 4×20 mL) and the combined organic fractions were washed with half-strength brine solution (40 mL), dried ($MgSO_4$), and the solvent was removed under reduced pressure to give a yellow solid. Subjection of the crude material to preparative RP-HPLC [gradient of 5–50 % acetonitrile (0.05 % TFA) in water (0.05 % TFA) over 50 min] gave the desired Dpa-functionalised trioxazole **6** (t_R = 30.3 min, 27 mg, 76 %) as a yellow oil. $[\alpha]_D^{20} = -49.0$ ($c = 1.0$, MeOH); ^{1}H NMR (400 MHz, CD_3OD): $\delta = 0.97$ (d, $J = 6.4$ Hz, 3H), 1.04 (d, J = 6.4 Hz, 3H), 1.73–2.12 (complex m, 11H), 3.11–3.29 (m, 4H), 4.50 (s, 8H), 5.20 (m, 2H), 5.29 (m, 1H), 7.61 (m, 4H), 7.69 (m, 4H), 8.10 (m, 4H), 8.45 (m, 3H), 8.60 (m, 1H), 8.72 ppm (m, 4H), two N-H signals not observed; ^{13}C NMR (100.6 MHz, CD_3OD): $\delta = 22.0$, 22.1, 22.9, 23.1, 25.9, 33.0, 33.2, 45.4, 45.5, 48.0(9), 48.1(3), 55.8, 58.3, 126.0, 126.3, 136.2(3), 136.2(5), 136.4, 142.0, 143.6, 143.7, 143.9, 148.2, 153.0, 161.2, 161.6, 161.7, 164.8, 164.9, 166.0 ppm, seven signals obscured or overlapping; HRMS (ESI) calcd. for $C_{49}H_{55}N_{12}O_6$ $[M+H]^+$ 907.4362, found 907.4343.

Acknowledgements

We thank the Australian Research Council for financial support and Dr C. E. Marjo (UNSW), Prof. S. Kable (USyd), and Assoc. Prof. T. Schmidt (USyd) for helpful discussions.

[1] L. Stryer, *Biochemistry*, *4th ed.*, W. H. Freeman and Company, New York, **1998**.
[2] R. D. Altman, O. E. Muniz, J. C. Pita, D. S. Howell, *Arthritis Rheum.* **1973**, *16*, 171–178; M. Doherty, C. Belcher, M. Regan, A. Jones, J. Ledingham, *Ann. Rheum. Dis.* **1996**, *55*, 432–436.
[3] L. V. Avioli, J. E. McDonald, R. A. Singer, *J. Clin. Endocrinol.* **1965**, *25*, 912; R. A. Terkeltaub, *Am. J. Physiol. Cell Physiol.* **2001**, *281*, C1–C11; R. G. G. Russell, S. Bisaz, A. Donath, D. B. Morhan, H. Fleisch, *J. Clin. Invest.* **1971**, *50*, 961–969; R. G. G. Russell, S. Bisaz, H. Fleisch, H. L. F. Currey, H. M. Rubenstein, A. A. Dietz, I. Boussine, R. Gabay, A. Micheli, G. Fallet, *Lancet* **1970**, *296*, 899–902.
[4] S. H. Moochhala, J. A. Sayer, G. Carr, N. L. Simmons, *Exp. Physiol.* **2007**, *93*, 43–49.
[5] L. Tang, Y. Li, H. Zhang, Z. Guo, J. Qian, *Tetrahedron Lett.* **2009**, *50*, 6844–6847; J. F. Zhang, S. Kim, J. H. Hae, S.-J. Lee, T. Pradhan, Q. Y. Cao, S. J. Lee, C. Kang, J. S. Kim, *Org. Lett.* **2011**, *13*, 5294–5297; P. Sokkalingam, D. S. Kim, H. Hwang, J. L. Sessler, C.-H. Lee, *Chem. Sci.* **2012**, *3*, 1819–1824.
[6] S. K. Kim, D. H. Lee, J.-I. Hong, J. Yoon, *Acc. Chem. Res.* **2009**, *42*, 23–31.
[7] J. Wen, Z. Geng, Y. Yin, Z. Zhang, Z. Wang, *Dalton Trans.* **2011**, *40*, 1984–1989; N. Shao, J. H. Wang, X. Gao, R. Yang, W. Chan, *Anal. Chem.* **2010**, *82*, 4628–4636.
[8] H. T. Ngo, X. Liu, K. A. Jolliffe, *Chem. Soc. Rev.* **2012**, *41*, 4928–4965.
[9] D. H. Lee, J. H. Im, S. U. Son, Y. K. Chung, J.-I. Hong, *J. Am. Chem. Soc.* **2003**, *125*, 7752–7753; D. H. Lee, S. Y. Kim, J.-I. Hong, *Angew. Chem.* **2004**, *116*, 4881–4884; *Angew. Chem. Int. Ed.* **2004**, *43*, 4777–4780; H. K. Cho, D. H. Lee, J.-I. Hong, *Chem. Commun.* **2005**, 1690–1692; J. H. Lee, A. R. Jeong, J.-H. Jung, C.-M. Park, J.-I. Hong, *J. Org. Chem.* **2011**, *76*, 417–423
[10] B. Ma, C. Meredith, H. F. Schaefer, III, *J. Phys. Chem.* **1994**, *98*, 8216–8223; M. E. Colvin, E. Evleth, Y. Akacem, *J. Am. Chem. Soc.* **1995**, *117*, 4357–4362.
[11] M. J. McDonough, A. J. Reynolds, W. Y. G. Lee, K. A. Jolliffe, *Chem. Commun.* **2006**, 2971–2973.
[12] S. Kubik, *Synthetic Peptide-Based Receptors*, in *Supramolecular Chemistry: From Molecules to Nanomaterials* (Eds.: J. W. Steed, P. A. Gale), Wiley, Hoboken, NJ, **2012**.
[13] K. A. Jolliffe, *Supramol. Chem.* **2005**, *17*, 81.
[14] S. J. Butler, K. A. Jolliffe, *Org. Biomol. Chem.* **2011**, *9*, 3471–3483.
[15] S. J. Butler, K. A. Jolliffe, W. Y. G. Lee, M. M. McDonough, A. J. Reynolds, *Tetrahedron* **2011**, *67*, 1019–1029.
[16] R. M. C. Dawson, D. C. Elliot, W. H. Elliot, K. M. Jones, *Data for Biochemical Research*, *3rd ed.*, Oxford, Clarendon Press, **1986**.
[17] J. Veliscek-Carolan, S. J. Butler, K. A. Jolliffe, *J. Org. Chem.* **2009**, *74*, 2992–2996.
[18] Z. J. Kamiński, B. Kolesińska, J. Kolesińska, G. Sabatino, M. Chelli, P. Rovero, M. Blaszczyk, M. L. Glówka, A. M. Papini, *J. Am. Chem. Soc.* **2005**, *127*, 16912.
[19] S. L. Wiskur, H. Ait-Haddou, J. J. Lavigne, E. V. Anslyn, *Acc. Chem. Res.* **2001**, *34*, 963; *Competition Experiments*, L. You, E. V. Anslyn in *Supramolecular Chemistry: From Molecules to Nanomaterials* (Eds.: J. W. Steed, P. A. Gale), Wiley, Hoboken, NJ, **2012**.
[20] R. G. Hanshaw, S. M. Hilkert, H. Jiang, B. D. Smith, *Tetrahedron Lett.* **2004**, *45*, 8721.
[21] All curve fitting was performed using the *Equilibria* program, C. E. Marjo, University of New South Wales Analytical Centre, Sydney, Australia; http://www.sseau.unsw.edu.au/Index.htm, **2009**.
[22] P. Thordarson "Binding Constants and Their Measurement" in *Supramolecular Chemistry: From Molecules to Nanomaterials*, DOI: 10.1002/9780470661345.smc018, Wiley, **2012**.

[23] K. A. Connors, *Binding Constants, Measurement of Molecular Complex Stability*, Wiley, New York, **1987**.
[24] N. A. Kuznetsova, O. L. Kaliya, *Russ. Chem. Rev.* **1992**, *61*, 683–696.
[25] R. K. Airas, *Biophys. Chem.* **2007**, *131*, 29–35.
[26] C. T. Burt, H.-M. Cheng, S. Gabel, R. E. London, *J. Biochem.* **1990**, *108*, 441–448.
[27] J. E. Wilson, A. Chin, *Anal. Biochem.* **1991**, *193*, 16–19.

Received: July 12, 2012
Published online: ■■ ▮▮, 0000

FULL PAPER

Mixing in different circles: Cyclic peptide-based receptors bind preferentially to pyrophosphate (PPi) over ATP, ADP, and phosphate in physiological saline (Krebs buffer). Selectivity for PPi over ATP and ADP is significantly enhanced in this biologically relevant fluid in comparison to that observed in water.

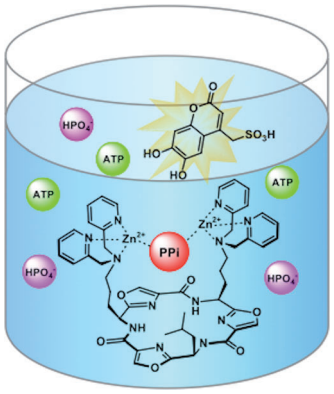

Molecular Recognition

Stephen J. Butler,
*Katrina A. Jolliffe** ———— ▮▮▮▮–▮▮▮▮

Selective Pyrophosphate Recognition by Cyclic Peptide Receptors in Physiological Saline